Uncertainty Analysis of a Loss of Cooling and Loss of Coolant Accident in a Spent Fuel Pool using TRACE

Francisco Sánchez-Sáez[a,*], Sofia Carlos[a], Jose Felipe Villanueva[a], Ana I. Sánchez[b], Sebastian Martorell[a]

[a] *Departamento de Ingeniería Química y Nuclear (Universidad Politécnica de Valencia)*
[b] *Departamento de Estadística e Investigación Operativa (Universidad Politécnica de Valencia)*

Abstract

Most of the uncertainty analyses in nuclear safety studies have been carried out for transients and accidents of the primary and secondary systems, but it is interesting to extend the analysis to other types of structures in a Nuclear Power Plant. In this work an uncertainty analysis of a loss of coolant and loss of cooling accident in a spent fuel pool is presented. The spent fuel pool has been modelled with TRACE V5.0 Patch 5 using a VESSEL 3D component in Cartesian coordinates. In addition, the model has been calibrated using Main Yankee spent fuel pool experimental data of temperatures and flows measured in steady state conditions. Using the calibrated model, the analysis of the accident was performed considering uncertainty in boundary conditions and in all the coefficients included in the TRACE uncertainty quantification data module. Then, Wilks' method and surrogate models were considered for evaluating the figure of merit of the accident. The figure of merit selected in this work is the time at which the cladding oxidation eaches 0.17 times the cladding thickness before oxidation (CFR 50.46 b2). The technique use to construct the surrogate model is the Elastic Net regression. The models were validated with cross validation and the results showed a good fit for the suggested models. Finally, the surrogate models are capable to predict in a few seconds an estimation of the available time until the limit is reached if the input variables are known. This is a great save in computational effort. In addition, the Elastic Net is able to identify most relevant variables, which are for the study transient: fuel and cladding specific heats, rod internal pressure coefficient, burst temperature coefficient, a group of fluid regime heat transfer coefficients, the cladding metal-water reaction rate coefficient and the cladding tolerance for the average cores.

Keywords: Spent Fuel Pool; TRACE; Elastic Net; LASSO regression; Uncertainty Analysis; Wilks.

1. Introduction

Mainly, uncertainty analysis (UA) in nuclear safety studies has been performed for primary and secondary system accidents and transients (D'Auria, 2017; D'Auria et al., 2012; Glaeser et al., 1994;

*Corresponding Author

Email addresses: frasansa@etsii.upv.es (Francisco Sánchez-Sáez), scarlos@iqn.upv.es (Sofia Carlos), jovillo0@upvnet.upv.es (Jose Felipe Villanueva), aisanche@eio.upv.es (Ana I. Sánchez), smartore@iqn.upv.es (Sebastian Martorell)

IAEA, 2008; Perez et al., 2011; Pourgol-Mohammad, 2009; Sánchez-Sáez et al., 2017, 2018; Wilson, 2013). However, it is interesting to extend the analysis further, to other kind of structures of the nuclear power plants, such as spent fuel pools (SFP). SFP keep spent fuel elements once they have accomplished their function in the reactor. Besides ionizing radiation, SFP elements also generate a considerable amount of heat due to the residual power, which has proven to be important for the safety conditions in some circumstances, as for example it was evidenced in Fukushima's accident.

In this paper, an accident involving loss of cooling plus loss of coolant through the transfer channel of Maine Yankee SFP is analyzed. This situation is considered as one of the possible beyond design basis accidents (Throm, 1989). The thermal-hydraulic model is constructed using TRACE code, which, although was created to analyze large/small break LOCAs and system transients in both pressurized- and boiling-water reactors, it has the capabilities to model TH phenomena in three-dimensional (3-D) space. Traditionally, the TH transient simulations for SFP have been done withcomputational fluid dynamics (CFD) codes (Chen et al., 2014; Hung et al., 2013; Oertel et al., 2019), but their computational costs are higher. For taking into account the uncertainty in simulation, a figure of merit (FOM) has to be defined, and in this case the time until cladding oxidation limit is selected to perform UA using Wilks' method and partial substitution of the TH model by surrogate models are used. The surrogate models have been obtained by multiple linear regression using penalized least squares throughout the Elastic Net.

The organization of the paper is as follows: section 2 introduces the accident simulated and the model constructed for Maine Yankee SFP are described. In Section 3 are presented the statistical techniques employed in the UA. In Section 4 the UA is carried out for the loss of cooling and loss of coolant accident. Finally, Section 5 presents the conclusions.

2. Loss of cooling and loss of coolant accident simulated at Maine Yankee SFP

2.1. System description

In this study, the UA methodology has been applied on a loss of cooling and loss of coolant in Maine Yankee SFP. When loss of cooling plus loss of coolant by the transfer channel transient of the SFP occurs and considering that there is no any additional safety system available to actuate, the accidental sequence follows the events shown in Figure 1.

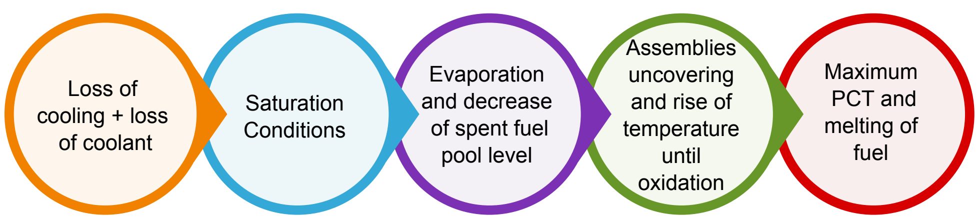

Figure 1: Events after the loss of SFP cooling system.

2.2. SNAP/TRACE model

In order to simulate the transient, the SFP model was built using TRACE code, which is shown in Figure 2. The TH model consists of a Cartesian 3D VESSEL, a FILL component, which simulates the inflow and two BREAK components, simulating the main outflow and the atmosphere.

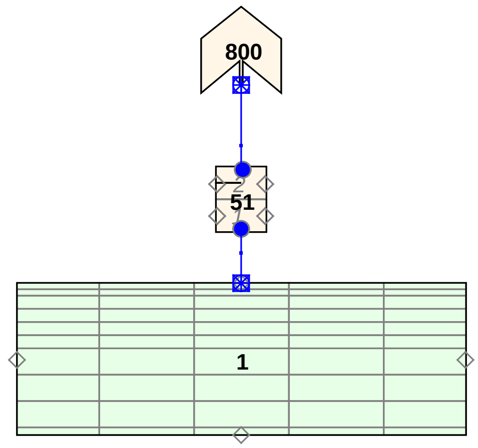

Figure 2: SNAP view of the Maine Yankee SFP TRACE model.

The X and Y coordinates of the Cartesian VESSEL were divided in 5 parts and the Z coordinate, which represents the SFP depth, was divided in 10 levels. Using this data, the complete VESSEL component has 250 cells. The length of each direction of the cells are presented in Table 1. The water volume in each VESSEL cell is not the same, as it depends on the number of spent fuel elements present in each location. Therefore, the area and volume fractions of the different cells were calculated according to the spent fuel elements distribution. The spent fuel elements range from Z=2 to Z=8. Above the elements, in Z=9 the SFP is full of water. At last, the Z=10 cells are full of air and simulate the SFP building.

Table 1: Nodes measures (m) of Vessel component.

Node	**X**	**Y**	**Z**
1	2.57	2.39	0.240
2	2.96	2.64	0.824
3	2.96	2.64	0.824
4	2.96	2.64	0.824
5	2.57	2.39	0.412
6			0.412
7			0.412
8			0.412
9			0.200
10			0.200

The residual power of the spent fuel elements was distributed throughout the pool by means of HEAT STRUCTURE components according to the Maine Yankee Licensing Case, using the data from Gay and colleagues (Gay, 1984; Gay and Gloski, 1983). In the Licensing Case, the SFP has all of his racks full of elements, with two different areas. One of such areas comprises 70 hot elements that generate a power of 4.8 MW and the other generates 1.6 MW. Therefore, the total amount of power inside the SFP is 6.4 MW. The power generated was simulated using two POWER components, each one of them connected to a HEAT STRUCTURE component. Further and more detailed results of the transient case (with another TRACE Version and another nodalization) can be found in Carlos et al. (2014).

3. Uncertainty Analysis methods

In order to perform a UA one or more FOM have to be selected depending on the transient to be analyzed. Then, the most interesting model parameters, which are being considered in the UA have to be identified. Finally a uncertainty quantification technique was to be applied to the response data obtained with the code. Wilks' method is the most extended technique used for TH simulations, among other reasons because a low number of code runs are needed to obtain a good estimation of tolerance limit.

3.1. Figure of merit

Based on the safety limits established by the CFR 50.46 (USNRC, 2007), three different candidates were considered to be FOM (Table 2).

Table 2: Safety variables, FOM and acceptance criteria based on CFR 50.46

Barrier	**Safety Variable**	**FOM**	**Acceptance Limit**
fuel	CR (calculated total oxidation of the cladding anywhere)	TMCR (time until MCR)	MCR (CR reaches 0.17 times the total cladding thickness before oxidation)
fuel	H2 (calculated total amount of hydrogen generated from the chemical reaction of the cladding with water or steam)	TMH2 (time until MH2)	MH2 (H2 reaches 0.01 times the hypothetical amount that would be generated if all of the metal in the cladding cylinders surrounding the fuel were to react)
fuel	PCT (calculated maximum fuel element cladding temperature)	TMPCT (time until MPCT)	MPCT (PCT reaches 1477K)

3.2. Uncertainty data for TRACE parameters

UA requires the selection of relevant input variables for the transient to allow the propagation of the uncertainty from the input variables to FOM. In this work, 37 variables included in the TRACE V5.0 Patch5 uncertainty quantification data module, which consists of a list of sensitivity coefficients (USNRC, 2017) were selected, as well as other 5 variables related to the fuel characteristics: Axial losses, Average pellet tolerance (Av pellet), Average cladding Inner tolerance (Av cladding), Hot core pellet tolerance (HC pellet) and Hot core cladding inner tolerance (HC cladding). These 5 variables have been found relevant in previous works (Feria and Herranz, 2017; Geelhood et al., 2009). The 37 variables of the TRACE module list of sensitivity coefficients, are distributed as U[0.9, 1.1] since their probability density functions are unknown. For the other uncertain variables, normal distributions are suposed. In particular, "Axial losses"" as N($\mu = 1$, $\sigma = 0.025$); "Av Pellet" and "HC Pellet"" (in mm) as N($\mu = 4.37$, $\sigma = 0.0065$); and "Av cladding" and "HC cladding" (in mm) as N($\mu = 4.47$, $\sigma = 0.02$), where the normal distributed variables are truncated to $\mu \pm 2\sigma$.

3.3. Uncertainty analysis using the Wilks' method

Wilks' method (Wilks, 1942, 1941) uses the order statistics as tolerance limits. Let X be a continuous random variable with a cumulative distribution function (CDF), $F_x(\cdot)$ and a simple random sample of size n of X. Let $X_{1:n} \leq X_{2:n} \leq \ldots \leq X_{r:n} \leq \ldots \leq X_{n:n}$ the order statistics from the sample. According to Wilks´ method the smallest number n of code runs to be performed to obtain the r-th order one-sided tolerance interval, or tolerance limit, of a particular FOM, is given by the following inequality:

$$1 - \sum_{k=n-r+1}^{n} \binom{n}{k} p^k (1-p)^{n-k} \geq \gamma \tag{1}$$

where p is the coverage probability and γ is the confidence level of the one-sided tolerance interval. It is common practice in BEPU applications, to use the 95/95 for the upper side (or 5/95 for the lower side) tolerance limit (p/γ) according to current regulatory practice. When first-order statistics (i.e. $r = 1$) is employed, it imposes the use of a sample size of 59 sets of TH input variables randomly selected from their pdf and performing 59 code runs, one for each set. However, in some cases first-order statistics can lead to very conservative results. Thus, applying the Wilks' formula to higher order statistics usually produces more accurate results but increases the computational burden, as more runs are needed. For example, if r is 2 and p/γ are 5/95, the minimum number of code runs needed to satisfy such criteria is $n = 93$. In this work, Wilks' method is used for $n = 93$ in order to estimate the tolerance limits of the FOM since a value of $n = 59$ gives very conservative results and $n > 93$ increases significantly the computational cost (Sánchez-Sáez et al., 2018).

3.4. Uncertainty analysis using surrogate models

The substitution of the TH code by a surrogate model for obtaining one or more FOM of interest is a technique employed in the simulation of the performance of complex systems and, particularly, in nuclear safety analysis (Carlos et al., 2013; Di Maio et al., 2016; Sánchez-Sáez et al., 2017), which allows performing a larger number of simulations with a reasonable computational cost and obtain the FOM of interest, instead of the whole system performance. So that, first FOM must be selected first appropriately. In this work, the technique proposed to undertake the UA is the Elastic Net regression, which is based on multiple linear regression where the coefficients are estimated by penalized least squares.

3.4.1. Ordinary least squares

Let standard multiple linear regression model, presented in Equation 2.

$$Y = \beta_0 + \sum_{j=1}^{p} \beta_j X_j + \epsilon. \tag{2}$$

Where Y is the observed dependent response variable (the FOM), and $\beta_0 + \sum_{j=1}^{p} \beta_j X_j$ is a linear combination of unknown parameters β and p independent variables X_j. The estimation of β coefficients can be done by ordinary least squares, which consists in minimize the Equation 3.

$$\sum_{i=1}^{n} (Y_i - \beta_0 - \sum_{j=1}^{p} \beta_j x_{ij})^2 \tag{3}$$

3.4.2. Elastic Net techniques

As an alternative to ordinary least squares, we can fit an Elastic Net model. Elastic Net consists of penalized least squares for obtaining the β parameters in multiple linear regression in order to reduce the model variance in spite of increasing the bias (Zou and Hastie, 2005). Elastic Net is useful when the number of predictors are elevated and the sample size is reduced as is in the work case.

With the objective of defining the Elastic Net, the 2 models on which it is based are described below. They are the Ridge regression (Kennard and Hoerl, 1970) and the LASSO (Least Absolute Shrinkage and Selection Operator) regression (Tibshirani, 1996).

Ridge regression. Ridge regression is very similar to ordinary least squares, except that the coefficients Ridge are estimated by minimizing a slightly different quantity. In particular, the Ridge regression coefficient estimates β are the values that minimize the Equation 4.

$$\sum_{i=1}^{n}(y_i - \beta_0 - \sum_{j=1}^{p}\beta_j x_{ij})^2 + \lambda\sum_{j=1}^{p}\beta_j^2, \tag{4}$$

where $\lambda \geq 0$ is a tuning parameter, to be determined separately. Equation {eq:ridge} trades off two different criteria. As with least squares, Ridge regression seeks coefficient estimates that fit the data well, by making the residual sum of squares, i.e. $\sum_{i=1}^{n}(y_i - \beta_0 - \sum_{j=1}^{p}\beta_j x_{ij})^2$, small. However, the second term, $\lambda\sum_j \beta_j^2$, called a shrinkage penalty, is shrinkage small when $\beta_1, ..., \beta_p$ are close to zero, and so it has the effect of shrinking penalty the estimates of β_j towards zero.

LASSO regression. LASSO regression is similar to Ridge, except for the penalization, which in this case is as is shown in Equation 5.

$$\sum_{i=1}^{n}(y_i - \beta_0 - \sum_{j=1}^{p}\beta_j x_{ij})^2 + \lambda\sum_{j=1}^{p} \mid \beta_j \mid \tag{5}$$

where $\lambda \geq 0$ is a tuning parameter, to be determined separately as in Ridge.

Elastic Net regression. For last, the Elastic Net is the joint between Ridge and LASSO so the parameters β_i are estimated by minimizing the Equation 6.

$$\sum_{i=1}^{n}(y_i - \beta_0 - \sum_{j=1}^{p}\beta_j x_{ij})^2 + \alpha(\lambda\sum_{j=1}^{p} \mid \beta_j \mid) + (1-\alpha)(\lambda\sum_{j=1}^{p}\beta_j^2), \tag{6}$$

where α determines the amount of LASSO and Ridge that contains the Elastic Net. When $\alpha = 1$ is exactly the LASSO and when $\alpha = 0$ we have the Ridge. In this work, the Elastic Net is constructed with R software (R-team, n.d.) using the library "glmnet" (Friedman et al., 2010).

3.5. Goodness of the surrogate model and cross-validation

When we have different models constructed with different techniques, or when we have multiple choices among the complexity of the models, we must provide some estimation of the goodness of the fit. One of the most employed estimators of the goodness of the fit is the mean squared error (MSE) between fitted and real values stated in Equation 7.

$$MSE = \frac{1}{n}\sum_{i=1}^{n}(y_i - \hat{y}_i)^2 \tag{7}$$

This estimator shows how good the fit of the sample is, but it does not say much about prediction. For estimate the goodness of the fit in terms of prediction, the Cross-Validation (CV) can be used (Kohavi, 1995). In particular, in this work the k-fold CV is used. It consists of splitting the data in k partitions, in order to hold the observations of one of the partitions for testing the model trained with the other $k-1$ partitions and average the test estimation for the k partitions. Therefore, the k-fold CV method is employed for selecting the tune parameters of the Elastic Net and for assessing the goodness of the fit out of sample (prediction) of the different techniques. In this case, moreover, the k selected is $k = 10$ based on Breiman and Spector (1992) and Kohavi (1995) since is recommended as a good compromise in the bias-variance tradeoff.

3.6. Probability density function

Wilks' method provides the tolerance limit of the FOM. Nevertheless, it is interesting to obtain more information about the behavior of the FOM, such as the probability density function (PDF). The PDF of the FOM can be estimated if the TH code runs sample is large enough (Carlos et al., 2013; Di Maio et al., 2016). But, when the runs sample is small, like in this study, it is necessary to search for alternatives. One of them relies on the surrogate models and feed them with a huge number of inputs (e.g. $N = 100000$) and obtain a pseudo-PDF of the FOM. With the pseudo-PDF we can obtain samples of $n = 93$ and obtain the tolerance limit as in Wilks' or an estimation of lower confidence interval for the percentile p calculated using the ranks showed in Equation 8 (Helsel and Hirsch, 2002).

$$R_l = np + z_{\gamma/2} \cdot \sqrt{np\,(1-p)} + 0.5 \tag{8}$$

Where n is the sample size, z is the standard normal distribution and $(1-\gamma)$ is the confidence level of the interval. The computed ranks, R_l and R_u are rounded to the nearest integers.

4. Results

4.1. Simulation results. Base case.

The base case considered is the simulation of the SFP model transient with all the variables in their nominal values. The evolution of the safety variables of interest, exposed in Table 2, related to their limits are shown in Figure 3, e.g. the ratio CR/MCR associated with the FOM of interest TMCR. The one that reaches its limit in the first place is the time when maximum cladding reacted (oxidation) percentage reaches the limit, TMCR, which occurs at 110256 s (30.63 hours). The next variable which reaches its safety limit is the hydrogen formation, at 112832 s (31.34 hours). Finally, the PCT reaches its limit at 113808 s (31.61 hours). Therefore, the TMCR is adopted as the FOM of this study.

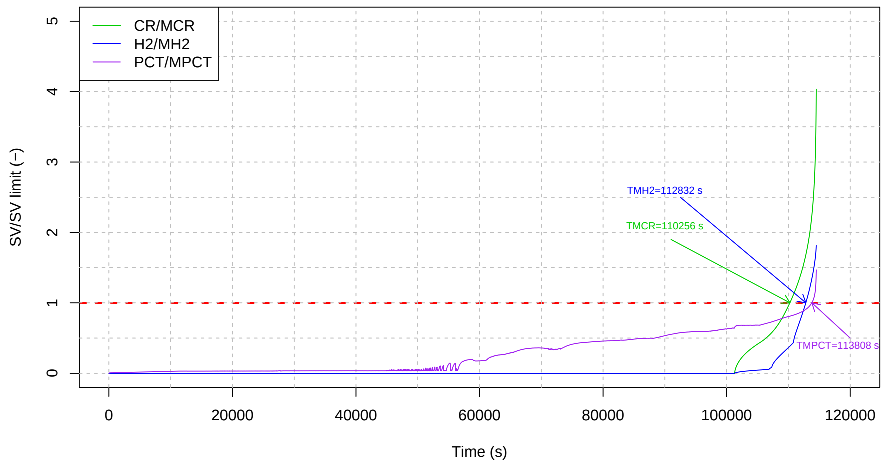

Figure 3: Evolution of FOM related to safety limits.

4.2. Results of the Uncertainty analysis

Using simple random sampling with the uncertain variables selected in this work and explained in 3.2, 93 TRACE simulations were run in order to perform the UA. Figure 4 shows the temporal evolution of the CR for the n=93 simulations. Specifically, in all the simulations the shape is the same but they are shifted. Figure 5 shows the information about TMCR for each simulation via box and whisker diagram.

4.2.1. Tolerance limit with Wilks' method

In order to estimate the value which covers the 5/95 tolerance limit, the Wilks' method was employed for the FOM. For the second order statistic ($n_2 = 93$) gives 109555 s (30.43 hours).

4.2.2. Elastic Net regression as surrogate model

In this section, two different Elastic Nets as surrogate model to obtain the TMCR are constructed and compared. These surrogate models address explicitly the effects of all the uncertainty variables on the FOM. However, only a set of the most relevant ones is identified once the surrogate model is built.

For the Elastic Net, it is necessary to tune parameters α and λ of Equation 6. In particular, the CV estimated error was calculated for 41 different and equidistant values of α, from 0 to 1. For each α, 500 CV repetitions were performed for choosing the λ optimum. In each of the repetitions of the CV, an error estimation curve was obtained for different values of λ. There are 2 different approaches for selecting the λ optimum value: the λ that minimizes the error, λ_{min} , or the λ that is one standard deviation from λ_{min}, the λ_{1se}. The median of the 500 CV repetitions errors are shown in Figure 7. The lowest error was reached with $\alpha = 0.95$ for the λ_{min} approach, and with $\alpha = 1$, which corresponds with the LASSO regression, for the λ_{1se} approach. The models with the selected values of α for both approaches were constructed (0.95, λ_{min}), (1.0, λ_{1se}). Figure 6 shows

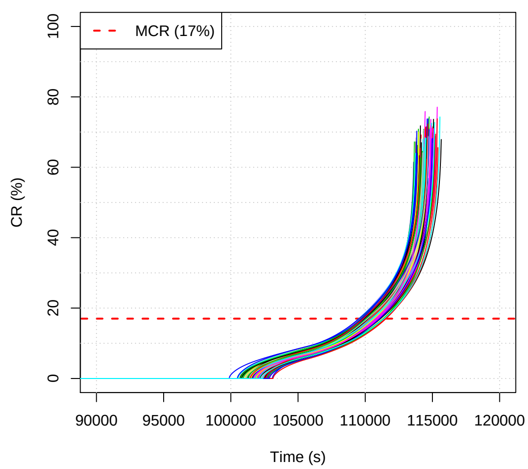

Figure 4: Evolution of the maximum oxidation in cladding of the SFP for the full model runs.

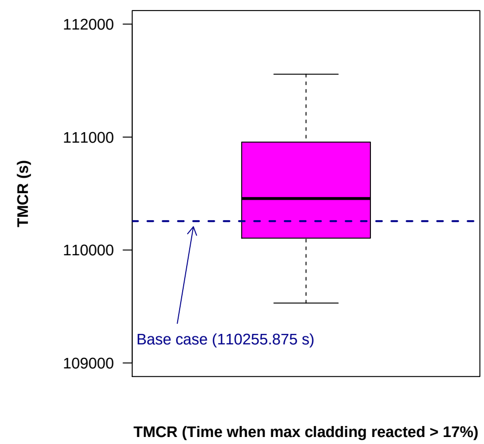

Figure 5: Time when maximum cladding reacted percentage is above the limit for the TH code simulations.

one of The CV repetition for the selected values of α. The λ_{min} and the λ_{1se} are highlighted with dotted lines. In addition, the number of variables depending on λ are indicated in the superior axis. It can be observed that with λ_{1se} approach a more parsimonious model is obtained.

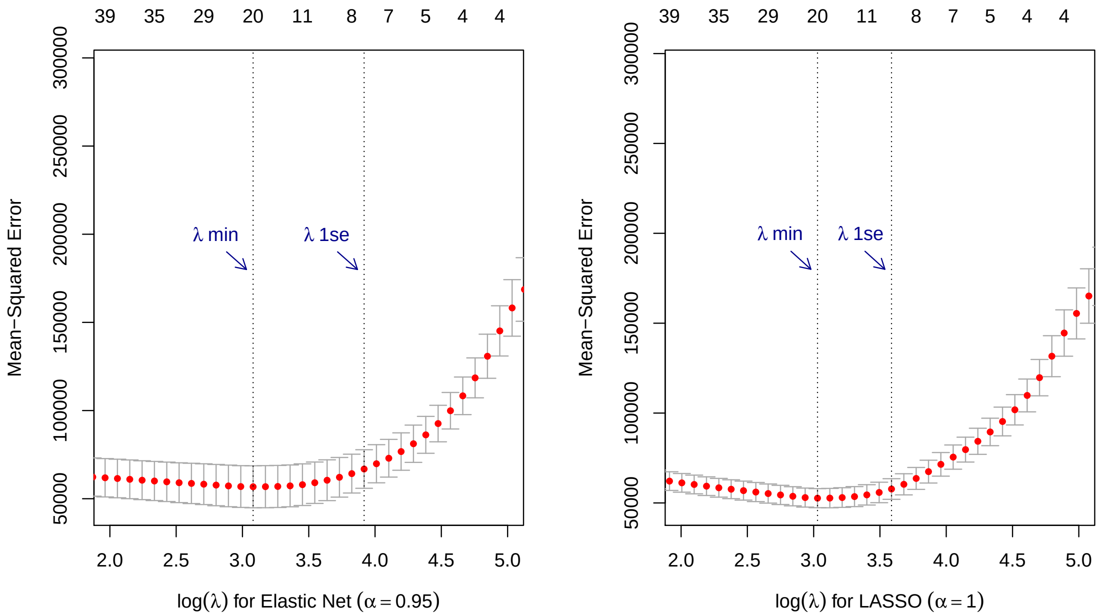

Figure 6: CV Error and coefficient values for Elastic Net regression models

Table 3 shows the β coefficients of each regression adjusted, as well as the values of the CV (root squared) errors for each method, λ_{min} and λ_{1se}. Taking into account these errors, the method that fits better is the Elastic Net with a λ_{min} approach, but the Elastic Net with a λ_{1se} is the most parsimonious model since it addresses 10 variables in comparison with the 14 variables for the first one. Moreover, the variables selected in both approaches were nested, as all the variables in the Elastic Net with λ_{1se} are included in the Elastic Net with λ_{min}.

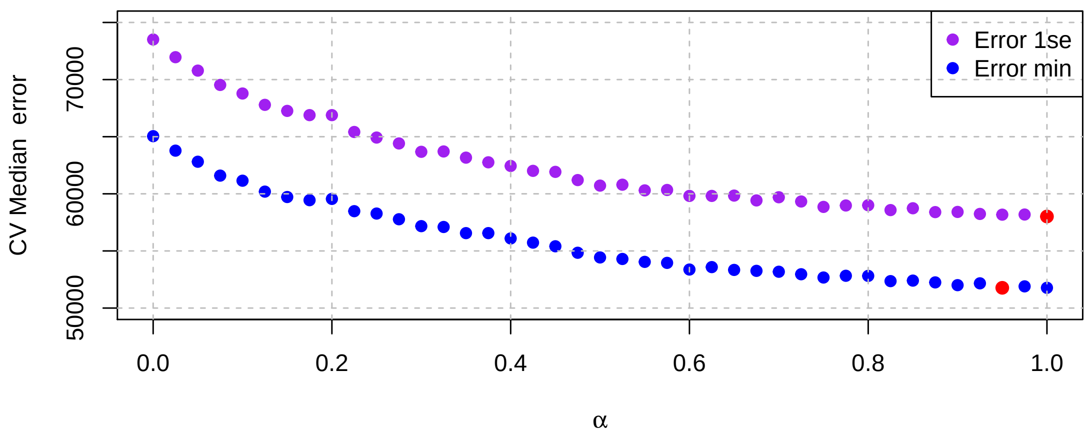

Figure 7: CV (k=10) median errors vs α

Table 3: Comparative of the regression models

Variable	Description	LASSO λ_{min}	LASSO λ_{1se}
(Intercept)		105290.5	104729.9
Av cladding	Average cladding tolerance	-6834453	-5935775.8
annMistLIHTCSV	Liquid to interface annular-mist heat transfer coefficient	-308	-39.2
bubSlugVIHTCSV	Vapor to interface bubbly-slug heat transfer coefficient	-130.9	
stratVIHTCSV	Vapor to interface stratified heat transfer coefficient	-46.1	
spLHTCWallSV	Single phase liquid to wall heat transfer coefficient	-30.3	
spVHTCWallSV	Single phase vapor to wall heat transfer coefficient	4996.9	4760.2
subcHTCWallSV	Subcooled boiling heat transfer coefficient	-729.2	-455.8
cladMWRxnRteSV	Cladding metal-water reaction rate coefficient	-2689.1	-2354.2
RodIntPressSV	Rod internal pressure coefficient	823.3	528.8
burstTempSV	Burst temperature coefficient	-1202	-901.1
bSlgVSIntDragSV	Interfacial drag (bubbly/slug Vessel) coefficient	47.2	
cladSpHtSV	Cladding Specific Heat	506.5	262.3
invAnnVWHTCSV	Vapor to wall inverted annular heat transfer coefficient	-267.2	-1.7
fuelSpHtSV	Fuel specific heat	4200	3937.2
CV RMSE		***228***	***241.6***
Variables		***14***	***10***

4.3. Safety tolerance limits obtained with the surrogate models

The surrogate models built can be used for predicting the response, the FOM, whatever the value adpopted by the relevant input variables. Furthermore, using a large set of input values of the variables, a pseudo-population that replicates the FOM of interest can be built. With 100000 different sets of input values the estimated PDF of the FOM is obtained, and showed in Figure 8). In addition, the 5th percentile confidence interval is calculated for each of the estimated pseudo-populations.

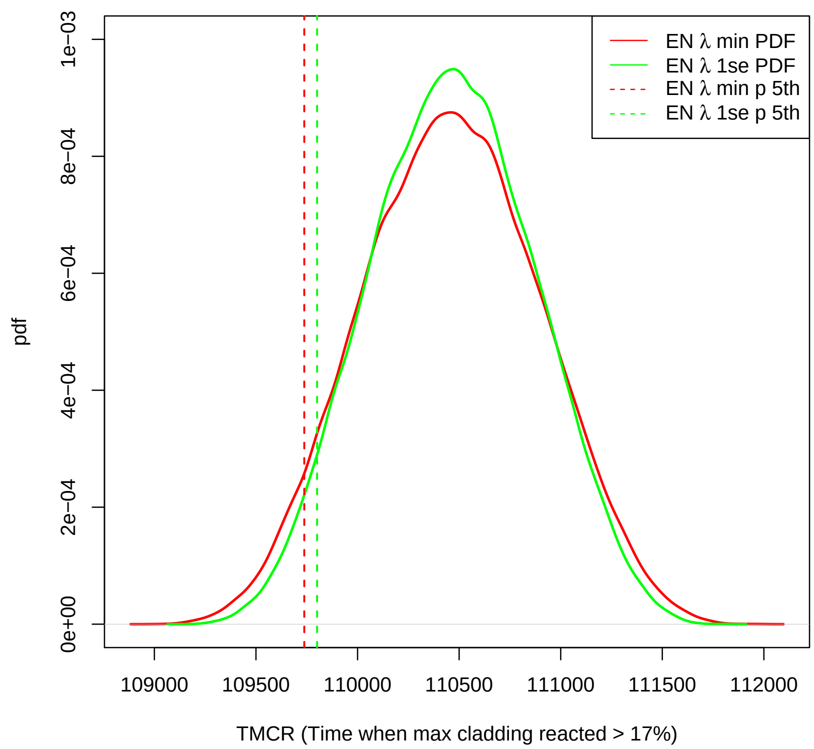

Figure 8: pdf estimated for the surrogate models

The tolerance limit 5/95 with the Wilks' method can be calculated. It is sampled n=93 FOM values for each of the 2 pseudo-population and the tolerance limit was estimated via order statistics. The process was repeated 1000 times in order to check the variability of the sampling. Figure 9 shows the tolerance limits predicted by both Elastic Nets. Moreover, they are compared with the TH code Wilks' estimations of the tolerance limit 5/95. The median values of the pseudo-population limits, in hours, are shown in Table 4. The estimations for the Elastic Net with a λ_{min} approach have a median value very similar to TH wilks' estimation. On the other hand. The estimations for the Elastic Net with λ_{1se} are slightly higher. Therefore, in the last case they are less conservative than the TH code Wilks' estimations.

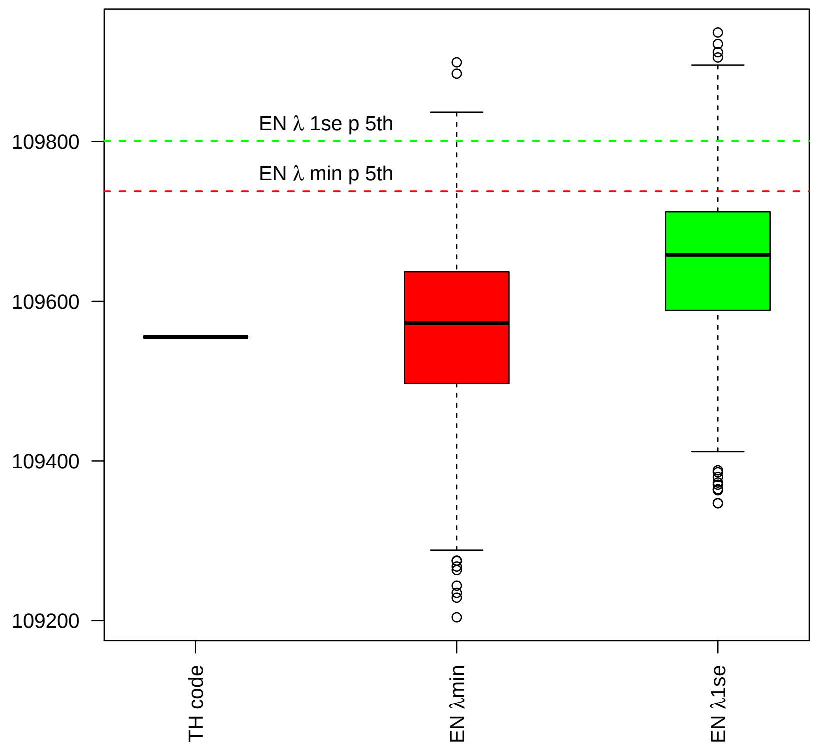

Figure 9: tolerance limits estimated from different populations/models

Table 4: Medians, in hours, of the tolerance limits estimated with order statistics

Population	**Second order statistic (h)**
Thermal Hydraulic Code	30.432
Elastic Net λ_{min}	30.437
Elastic Net λ_{1se}	30.461

5. Conclusion

In this paper, uncertainty analysis of a loss of cooling and loss of coolant accident in a SFP was performed. The 5/95 tolerance limit with the Wilks' method was obtained using second order statistic (i.e. $n = 93$). This time available, since the transient starts, until the maximum cladding reacted exceeds 17%, i.e. TMCR, was 30.432 hours.

In addition, the $n = 93$ simulations of the TH code were used to build two surrogate models, based on Elastic Nets, with which the 5/95 limits have also been obtained. With these models, the tolerance limits were close to those obtained with the TH code simulations.

The choice of the method for constructing the surrogate model depends on the particular objectives of the study. The different techniques have a similar performance. The best model in terms of number of variables was the Elastic Net with a λ_{1se} approach, while the best model according to the CV error was the Elastic Net with a λ_{min} approach. From the 42 initial uncertain variables (37 from TRACE sensitivity module and 5 external), with Elastic Net with a λ_{min} approach they have been reduced to 14 (13 from TRACE module and 1 external). With the Elastic Net with a λ_{1se}, the number of relevant variables is reduced even more, to 10 (9 from TRACE module and 1 external). TRACE module relevant variables, are related with the fuel charactheristics (fuel and cladding specific heats, rod internal pressure coefficient and burst temperature coefficient), heat transfer coefficients and the cladding metal-water reaction rate coefficient. The only one external relevant variables is the cladding tolerance for the average cores.

Finally, the surrogate models are capable to predict in a few seconds an estimation of the available time until the limit is reached if the input variables are known. This is a great save in computational effort as the TH code spends 21 hours, in average, for each simulation. In addition, only the relevant input parameters need to be given attention in a more accurate way based on the particular surrogate model built.

Acknowledgments

The authors are grateful to the Spanish "Consejo de Seguridad Nuclear (CSN)" for the financial support they provided for Research MASA Project 2 and STN/4524/2015/640 (CAMP Project).

References

Breiman, L., Spector, P., 1992. Submodel selection and evaluation in regression. the x-random case. International Statistical Review / Revue Internationale de Statistique 60, 291–319.

Carlos, S., Sanchez-Saez, F., Martorell, S., 2014. Use of TRACE best estimate code to analyze spent fuel storage pools safety. Progress in Nuclear Energy 77, 224–238. https://doi.org/10.1016/j.pnucene.2014.07.008

Carlos, S., Sánchez, A., Ginestar, D., Martorell, S., 2013. Using finite mixture models in thermal-hydraulics system code uncertainty analysis. Nuclear Engineering and Design 262, 306–318.

Chen, S.R., Lin, W.C., Ferng, Y.M., Chieng, C.C., Pei, B.S., 2014. Development of 3-d cfd methodology to investigate the transient thermal-hydraulic characteristics of coolant in a spent fuel pool. Nuclear Engineering and Design 275, 272–280.

Di Maio, F., Bandini, A., Zio, E., Alberola, S.C., Sanchez-Saez, F., Martorell, S., 2016. Bootstrapped-ensemble-based sensitivity analysis of a trace thermal-hydraulic model based on a limited number of pwr large break loca simulations. Reliability Engineering & System Safety 153, 122–134.

D'Auria, F., 2017. 14 - best-estimate plus uncertainty (bepu) approach for accident analysis, in: Thermal-Hydraulics of Water Cooled Nuclear Reactors. Woodhead Publishing, pp. 905–950.

D'Auria, F., Camargo, C., Mazzantini, O., 2012. The best estimate plus uncertainty (bepu) approach in licensing of current nuclear reactors. Nuclear Engineering and Design 248, 317–328.

Feria, F., Herranz, L.E., 2017. Application of the bepu methodology to assess fuel performance in dry storage. Annals of Nuclear Energy 99, 240–246.

Friedman, J., Hastie, T., Tibshirani, R., 2010. Regularization paths for generalized linear models via coordinate descent. Journal of Statistical Software 33, 1–22.

Gay, R., 1984. Spent nuclear fuel storage pool thermal hydraulic analysis. Progress in Nuclear Energy 14, 199–225.

Gay, R., Gloski, D., 1983. Verification of the gflow computer code using experimental data from the maine yankee spent-fuel storage pool (technical report No. 3097). EPRI NP.

Geelhood, K.J., Luscher, W.G., Senor, D.J., Cunningham, M.E., Lanning, D.D., Adkins, H.E., 2009. Predictive bias and sensitivity in nrc fuel performance codes. United States.

Glaeser, H., Hofer, E., Kloos, M., Skorek, T., 1994. Uncertainty and sensitivity analysis of a post-experiment calculation in thermal hydraulics. Reliability Engineering & System Safety 45, 19–33.

Helsel, D.R., Hirsch, R.M., 2002. Statistical methods in water resources techniques of water resources investigations, book 4. U.S. Geological Survey.

Hung, T.-C., Dhir, V.K., Pei, B.-S., Chen, Y.-S., Tsai, F.P., 2013. The development of a three-dimensional transient cfd model for predicting cooling ability of spent fuel pools. Applied Thermal Engineering 50, 496–504.

IAEA, 2008. Best estimate safety analysis for nuclear power plants, safety reports series no. 52. uncertainty evaluation. International Atomic Energy Agency, Vienna.

Kennard, R.W., Hoerl, A.E., 1970. Ridge regression: Biased estimation for nonorthogonal problems. Technometrics 12, 55–67.

Kohavi, R., 1995. A study of cross-validation and bootstrap for accuracy estimation and model selection, in: Proceedings of the 14th International Joint Conference on Artificial Intelligence - Volume 2, IJCAI'95. Morgan Kaufmann Publishers Inc., San Francisco, CA, USA, pp. 1137–1143.

Oertel, R., Hanisch, T., Krepper, E., Lucas, D., Rüdiger, F., Fröhlich, J., 2019. Two-scale cfd analysis of a spent fuel pool involving partially uncovered fuel storage racks. Nuclear Engineering and Design 341, 432–450.

Perez, M., Reventos, F., Batet, L., Guba, A., Tóth, I., Mieusset, T., Bazin, P., Crécy, A. de, Borisov, S., Skorek, T., Glaeser, H., Joucla, J., Probst, P., Ui, A., Chung, B.D., Oh, D.Y., Pernica, R., Kyncl, M., Macek, J., Manera, A., Freixa, J., Petruzzi, A., D'Auria, F., Del Nevo, A., 2011. Uncertainty and sensitivity analysis of a lbloca in a pwr nuclear power plant: Results of the phase v of the bemuse programme. Nuclear Engineering and Design 241, 4206–4222.

Pourgol-Mohammad, M., 2009. Thermal-hydraulics system codes uncertainty assessment: A review of the methodologies. Annals of Nuclear Energy 36, 1774–1786.

R-team, n.d. R: The R Project for Statistical Computing.

Sánchez-Sáez, F., Carlos Alberola, S., Villanueva, J.F., Sanchez Galdón, A.I., Martorell Alsina, S., 2017. Uncertainty analysis of pkl sbloca g7.1 test simulation using trace with wilks and gam surrogate methods. Nuclear Engineering and Design 319, 61–72.

Sánchez-Sáez, F., Sánchez, A.I., Villanueva, J.F., Carlos, S., Martorell, S., 2018. Uncertainty analysis of a large break loss of coolant accident in a pressurized water reactor using non-parametric methods. Reliability Engineering and System Safety 174, 19–28.

Throm, E.D., 1989. Regulatory analysis for the resolution of generic issue 82, "beyond design basis accidents in spent fuel pools" (No. NUREG–1353). United States.

Tibshirani, R., 1996. Regression Selection and Shrinkage via the Lasso. Journal of the Royal

Statistical Society. Series B (Methodological) 58, 267–288.

USNRC, 2017. TRACE v5.0 patch 5 user's manual volumes 1 and 2.

USNRC, 2007. Acceptance criteria for emergency core cooling systems for light-water nuclear power reactors (10 CFR 50.46). U.S. Nuclear Regulatory Commission, Washington, DC.

Wilks, S.S., 1942. Statistical prediction with special reference to the problem of tolerance limits. The Annals of Mathematical Statistics 13, 400–409.

Wilks, S.S., 1941. Determination of sample sizes for setting tolerance limits. The Annals of Mathematical Statistics 12, 91–96.

Wilson, G.E., 2013. Historical insights in the development of best estimate plus uncertainty safety analysis. Annals of Nuclear Energy 52, 2–9.

Zou, H., Hastie, T., 2005. Erratum: Regularization and variable selection via the elastic net. Journal of the Royal Statistical Society. Series B: Statistical Methodology 67, 301–320. https://doi.org/10.1111/j.1467-9868.2005.00527.x